The Self-Healing Performance of Carbon-Based Nanomaterials Modified Asphalt Binders Based on Molecular Dynamics Simulations

Yan Gong[1]*, Jian Xu[1], Er-hu Yan[1] and Jun-hua Cai[2]

[1]Research Institute of Highway, Ministry of Transport, Beijing, China, [2]Sanming Puyan Expressway Group Corporation, Fujian, China

In this study, the molecular dynamics simulation was used to explore the effects of carbon-based nanomaterials as binder modifiers on self-healing capability of asphalt binder and to investigate the microscopic self-healing process of modified asphalt binders under different temperature. An asphalt average molecular structure model of PEN70 asphalt binder was constructed firstly. Further, three kinds of carbon-based nanomaterials were added at three different percentages ranging from 0.5 to 1.5% to the base binder to study their effects on the self-healing capability, including two carbon nanotubes (CNT1 and CNT2) and graphene nanoflakes. Combining with the three-dimensional (3D) microcrack model to simulate the asphalt self-healing process, the density analysis, relative concentration analysis along OZ direction, and mean square displacement analysis were performed to investigate the temperature sensitive self-healing characters. Results showed that the additions of CNTs were effective in enhancing the self-healing efficiency of the plain asphalt binder. By adding 0.5% CNT1 and 0.5% CNT2, about 652% and 230% of the mean square displacement of plain asphalt binder were enhanced at the optimal temperatures. However, the use of graphene nanoflakes as an asphalt modifier did not provide any noticeable changes on the self-healing efficiency. It can be found that the self-healing capability of the asphalt was closely related to the temperature. For base asphalt, the self-healing effect became especially high at the phase transition temperature range, while, for the modified asphalt, the enhancement of the self-healing capability at the low phase transition temperature (15°C) became negligible. In general, the optimal healing temperature range of the CNTs modified asphalt binders is determined as 45–55°C and the optimal dosage of the CNTs is about 0.5% over the total weight of the asphalt binder. Considering the effect of carbon-based nanomaterials on the self-healing properties, the recommended carbon-based nanomaterials modifier is CNT1 with the aspect ratio of 1.81.

Keywords: molecular dynamics, self-healing, carbon-based nanomaterials, asphalt binder, optimal healing temperature

INTRODUCTION

In recent decades, the traffic load supported by asphalt road pavements has significantly increased. At the same time, the climate change has caused a wide range of temperature variations throughout the year, and the weather has become more extreme. These conditions lead to the need for the modification of base asphalt to improve the performance of the material and enhance the mechanical response of road pavements under the severe service conditions (for example, adhesion, temperature sensitivity, oxidation resistance, aging and oxidation resistance, self-healing, and durability). Many kinds of additives have been used as asphalt modifier, including resins, rubbers, polymers, sulfur, metal complexes, fibers, and chemical reagents, especially the most widely applied polymer modifiers with the excellent elastic and thermoplastic properties (Yildirim, 2007; Shen, 2011; Guo et al., 2020). However, most polymer modifiers are thermodynamically incompatible with asphalt binders. This may cause the composite to delaminate during thermal storage and reduce the performance of the modified asphalt. Therefore, the development of new asphalt materials has attracted a lot of attention to avoid the premature performance degradation and ensure a longer service life of the asphalt road pavements. And nanotechnology has gradually been introduced into the field of modified asphalt. Since the microstructure determines macroscopic performance, nanomodified asphalt provides a significant improvement in the intrinsic properties, which is different from other common asphalt modification methods. In order to enhance the mechanical properties and functional applications of asphalt materials, various nanomaterials are used in the laboratory to enhance the performance characteristics of asphalt mixtures (Steyn, 2009; Zare-Shahabadi et al., 2010; Fang et al., 2013; Yao et al., 2013).

Nanomaterials have the morphological characteristics on the nanoscale, especially the special properties related to the nanoscale dimensions. In this respect, carbon-based nanomaterials, which are represented by graphene (Novoselov et al., 2004) and carbon nanotubes, have opened up many new research fields in construction engineering. On the one hand, the addition of carbon-based nanomaterials can enhance the mechanical properties of mixtures, such as the stiffness and strength of mixtures (Young et al., 2012; Du and Pang, 2015b). On the other hand, since the graphene nanoflakes (GNF) and the carbon nanotubes (CNT) have the large specific surface area, strong antioxidant characteristics, high stability, high electric and thermal conductivity, and good mechanical properties, they can be used to improve the functional and smart road pavements (Du and Pang, 2015a; Lee et al., 2017). Besides, it has been proved that the carbon-based nanomaterials can react with the hydrophobic nonpolar groups in asphalt binder and then form more stable nanocomponents, which could act as the buffers for connecting the asphalt binder and the nanoparticle and offer a continuous transition of stress (Cheng et al., 2011; Liu et al., 2014). Thus, the carbon-based nanomaterials provide the possibility to realize more durable and smarter asphalt pavements. However, it must be noted that there are great differences in the chemical composition and mechanical properties of the nanomaterials and the pavement materials, such as the asphalt binders and the aggregates. Therefore, many efforts have been made to adapt the nanomaterials to the construction of more efficient and functional road infrastructures.
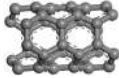
The carbon-based nanomaterials used as modifiers can improve the mechanical properties of pavement materials. Latifi and Hayati (Latifi and Hayati, 2018) reported that the addition of CNTs resulted in an enhancement in the stiffness, rutting resistance, and fatigue performance of hot mix asphalt, with the CNTs' optimum weight percentage of 1%. Faramarzi et al., (2011) found that the asphalt concrete adding CNTs showed improved Marshall stability compared to plain asphalt concrete. Wang et al., (2016) investigated the microwave healing performance of electrically conductive carbon fiber modified asphalt mixture beams and verified a partial recovery and healing process of cracked asphalt concrete with carbon fibers. In terms of self-healing performance, some studies have demonstrated that the application of induction heating was effective for healing cracks in asphalt mixture. Taking advantage of the large heat conductivity, the presence of CNT and GNF could modify the thermal conductivity of asphalt and its mixture, which will benefit to obtain the good self-healing and microwave healing effects. In Liu's study, the optimum heating temperature of 85°C was suggested to achieve the best healing effect (Liu et al., 2012). In addition, completely failed asphalt concrete was partially self-healed based on carbon materials added and induction heating method (Yoo et al., 2019). And the best healing capability was obtained for the specimens with 0.5% GNFs and CFs. Su et al., (2019) developed an improved mechanical properties set-up named the beam on elastic foundation to evaluate the self-healing efficiency of asphalt binder. The asphalt samples with graphene microcapsules containing oily rejuvenator were proved to keep a higher self-healing efficiency after five healing cycles under low temperature (Su et al., 2019) because of the high thermal conductivity of graphene. Based on this review, the positive effect of GNFs and CFs on asphalt binders has been demonstrated. However, there were varying trends in the obtained results because of affecting parameters such as the test temperature, the processing method, and the dosage of GNF and CF.

Nanotechnology testing methods are important for understanding asphalt modification. Molecular dynamics (MD) simulation is a modeling technique to simulate the atomic movements and dynamic behavior at nanoscale, which is widely applied to study the chemical interaction mechanism in road materials. The atoms and molecules move obeying the basic physical principles, Newton's law of mechanics, which are decided by the force field in the simulations (Maginn and Elliott, 2010). Actually, MD simulation is a powerful tool for understanding the macroscopic and intrinsic character of asphalt binders from the molecular scale, such as the physicochemical properties, the aging, and the bond energy of the asphalt-aggregate interface (Yao et al., 2016; Wang et al., 2017; Xu and Wang, 2017). In 2010, the healing analysis of asphalt

TABLE 1 | Properties of PEN70 asphalt binder.

Asphalt binders	Penetration (25°C), 0.1 mm	Softening point, °C	Ductility (15°C), cm	Viscosity (60°C), Pa·s
PEN70	68	47.0	>100	272.5

TABLE 2 | Lattice structure and physical properties of the carbon-based nanomaterials.

Nanomaterials	(m, n, k)	Chemical formula	Diameter, Å	Length, Å	L/D	Lattice structure
CNT1	(3, 0, 1)	C_{12}	2.35	4.26	1.81	
CNT2	(3, 3, 1)	C_{12}	4.07	2.46	0.60	
GNF	(-, -, 1)	C_{13}	500–2,000	—	—	

binders was firstly investigated using MD simulation by Bhasin et al., (2010). Recently, Sun et al., (2018) constructed a three-dimensional (3D) microcrack model with 20 Å crack and used MD simulations to explain the microscopic process of asphalt self-healing and investigate the self-healing capability of neat asphalt binders at different temperatures [26].

Although a lot of effort has been made to improve the durability of pavement materials and to enhance the self-healing capability in recent years as mentioned above, limited works have been conducted to understand the self-healing character of asphalt binders by using MD simulation. Investigating the interaction between asphalt binder and carbon-based nanomaterials, which could help in understanding the effect of carbon-based nanomaterials on the self-healing properties of asphalt binders, is still lacking. Furthermore, the determination of the suitable type and dosage of carbon material and the selection of the optimal induction heating temperature are not clear. Thus, in this study, the effectiveness of using three different types of carbon-based nanomaterials (CNT1, CNT2, and GNF) on improving the self-healing performance of asphalt binder was investigated. The average molecular structure models of the PEN70 asphalt binder were firstly constructed based on the measured structure parameters through a series of physical chemical experiments. Then, based mainly on MD simulations, the temperature sensitive self-healing character of damaged asphalt binders with and without carbon-based nanomaterials was quantitatively estimated under different temperature conditions. Lastly, the self-healing character of asphalt binders was analyzed to determine the suitable type and dosage of carbon material and the optimal heating temperature for self-healing.

MATERIALS

Asphalt Binders

In this study, the asphalt binder with the penetration grade of 70 (named PEN70) was selected to construct the corresponding average molecular model and investigate the temperature sensitive self-healing performances. The basic physical properties of the asphalt binder are shown in **Table 1**.

Carbon-Based Nanomaterials

Two types of carbon-based nanomaterials (CNT and GNF) were used as the modifiers in the PEN70 asphalt binder to enhance the mechanical properties and achieve the self-healing capacity. According to the diameter and length, two kinds of CNTs were adopted to investigate the effect of aspect ratio (L/D) on the self-healing performance of the asphalt binder. Herein, L and D are the length and the diameter, respectively. Meanwhile, the nanomaterials were added at three different weight percentages ranging from 0.5% to 1.5% to the base asphalt. The lattice structure and physical properties of the carbon-based nanomaterials are listed in **Table 2**. Their scanning electron microscope images had been shown in the previous study (Yoo et al., 2018; Yoo et al., 2019).

The CNT1 and CNT2 have the same chemical formula but different aspect ratio depending on how the carbon atomic layer sheet is rolled up. The GNF is a kind of two-dimensional nanomaterial composed of carbon atoms, which form hexagonal honeycomb lattice. Mostly, the GNF fibers used in industry were the multiple graphene films with a larger diameter than CNTs rather than the single ones because of the high prices

TABLE 3 | Average molecular structure parameters of PEN70 asphalt binder.

Structure parameters	PEN70
Molecular weight	1,406
Atomicity	241
Chemical formula	$C_{99}H_{138}N_1O_2S_1$
C_T	99
C_A	35
C_N	13
C_P	51
C_α	8.5
C_{AP}	18
C_I	17
H_T	138
H_A	9
H_α	17
H_β	83.5
H_γ	28
R_T	13.5
R_A	9.5
R_N	4

C, H, and R stand for the number of carbon atoms, hydrogen atoms, and rings, respectively. T, A, and N stand for the total, the aromatic, and cycloalkyl ones, respectively. C_α stands for the number of α carbon atoms of aromatic rings. C_{AP} and C_I stand for the number of carbon atoms around and inside aromatic rings. C_F stands for the number of carbon atoms of periconsensed aromatic rings. H_α, H_β, and H_γ stand for the number of hydrogen atoms attached to α carbon, β carbon, and γ carbon of aromatic rings, respectively.

and low industrial production of the single layer GNF. But in this paper, a single atomic layer graphene was constructed based on MD simulation method to analyze the enhancement effect on the self-healing capacity, as shown in **Table 2**. Note that the superlayer graphene also suffered the geometry optimization process due to the selected superlattice period.

SIMULATION MODELS

Average Molecular Structure Model of Asphalt

To achieve the average molecular structure model of PEN70 asphalt binder, a series of investigations were conducted, including the elemental analyzer, gel permeation chromatography, and proton nuclear magnetic resonance (^{1}H-NMR). The elements C, H, N, and S contents were calculated by a Vario EL-III elemental analyzer. And the structure parameters, including molecular weights, atomicity, and chemical formula, were obtained by gel permeation chromatography and element compositions. AVANCE-III HD500 (Bruker) was adopted to get the proton nuclear magnetic resonance (^{1}H-NMR) spectra, which identified the chemical shifts and distribution of hydrogens atoms. Based on these experiment results, the number of aromatic carbon atoms, naphthenic carbon atoms, and alkane branched chain carbon atoms was calculated according to the improved B-L methods (Katayama et al., 1975). The main structure parameters of PEN70 asphalt binder are listed in **Table 3**.
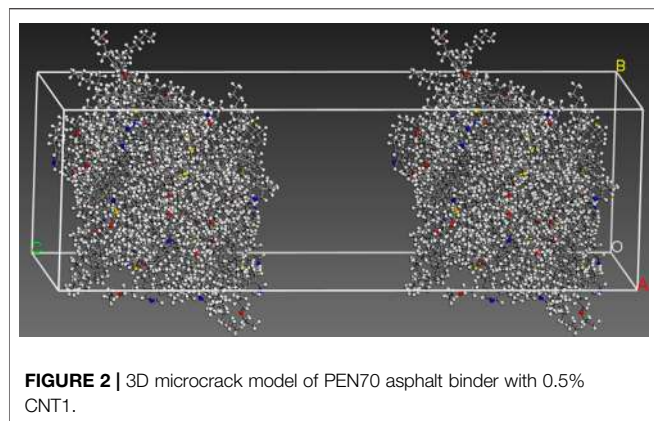
As shown in **Figure 1**, the average molecular structure model of PEN70 asphalt binder was constructed in the software
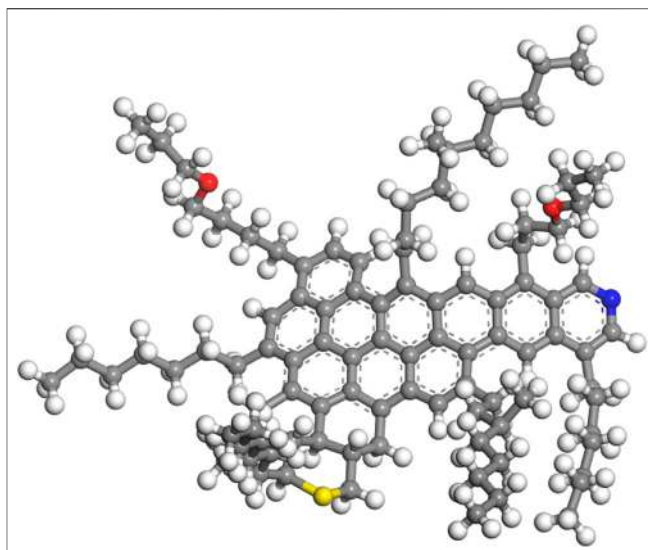
FIGURE 1 | Average molecular structure model of PEN70 asphalt binder.

Materials Studio 8.0, the specific construction process of which was not repeated in this article. More detailed information could be found in the author's other paper (Gong et al.). The dark gray and white atom, respectively, stand for carbon and hydrogen. The colored atoms represent different heteroatoms (the yellow one stands for sulfur, the red one stands for oxygen, and the blue one stands for nitrogen).

Using amorphous cell module, a bulk asphalt binder model was subsequently constructed, including the base PEN70 asphalt and the carbon-based nanomaterials modified asphalt. For the base PEN70 asphalt binder, the bulk system consisted of 20 average asphalt molecules, while, for the carbon-based nanomaterials modified asphalts, the modifiers were added in the bulk base asphalt system, and the amount depended on the molecular weight and the weight percentage of the modifiers. Taking the 1.5% CNT1 bulk modified asphalt for example, it consisted of 20 average PEN70 asphalt molecules and three CNT1 molecules. The initial densities of the cubic lattice of the bulk asphalt binder models were both set as 0.1 g/cm^3 for each binder. Then, the bulk asphalts were stabilized by processing the geometry optimization, canonical (NVT) ensemble simulation, and isothermal-isobaric (NPT) ensemble simulation in Forcite module to gradually reduce the total energy. In the geometry optimization simulation, the molecules in the bulk systems were subjected to 5,000 iterations of energy minimization by smart algorithm. The cutoff distance of the van der Waals terms was 12.5 Å. The NPT and NVT ensemble simulations were both performed with a time step of 1 fs ($10^{-15\,s}$) and a total time of 150 ps ($10^{-12\,s}$). The temperature was 298.15 K (25°C) and the pressure was 1.01×10^{-4} GPa.

When obtaining the final densities from the NPT ensemble simulation, the confined asphalt layers were reconstructed. Similarly, all the confined asphalt layers suffered the geometry optimization, NVT ensemble, and NPT ensemble

FIGURE 2 | 3D microcrack model of PEN70 asphalt binder with 0.5% CNT1.

FIGURE 3 | Density curve during self-healing (PEN70 asphalt binder with 1.5% CNT1, 55°C).

simulation to achieve the flat surface for the self-healing molecular models.

Self-Healing Molecular Model

The 3D microcrack model was constructed by positioning the confined asphalt layer-3 on the confined asphalt layer-1 through Build Layer module. A vacuum layer-2 with a thickness of 20 Å was added between two asphalt layers. The 3D microcrack model is showed in **Figure 2**, taking 0.5% CNT1 modified asphalt as an example. The volume parameter of the amorphous cell (0.5% CNT1) was 35.9 Å^3 × 35.9 Å^3 × 89.7 Å^3. To investigate the self-healing characters, the MD simulation was selected to in this section simulate the interactions and molecular movements at the 3D microcrack interface models. In simulation systems, the Universal forcefield and NPT ensemble were applied for the analysis of self-healing capability. The simulated temperature was set within 15–55°C, including 288.15 K (15°C), 298.15 K (25°C), 308.15 K (35°C), 318.15 K (45°C), and 328.15 K (55°C).

RESULTS AND DISCUSSION

Density Analysis

The dynamics simulation of the 3D microcrack model was conducted, and the volume parameter of the amorphous cell changed to 34.58 Å^3 × 34.58 Å^3 × 86.36 Å^3 after 150 ps (PEN70 asphalt binder with 0.5% CNT1). The density analysis simulation was further carried out. The density curve varying with time was shown in **Figure 3**, taking PEN70 asphalt binder with 0.5% CNT1 as an example. The initial density was 0.81 g/cm^3. With the increase of time, the density increased. After 100 ps, the density value tended to be stabilized at 0.91 g/cm^3, which was very close to that of the undamaged PEN70 asphalt binder with 0.5% CNT1, as shown in **Table 4**. The 3D microcrack model results showed that the healing behavior of the carbon-based nanomaterials modified PEN 70 asphalt could occur spontaneously over time.

In fact, based on the polymer self-healing theory, the discontinuity in materials can be automatically eliminated through the molecular wetting and diffusion process between the discontinuous interfaces, which is called self-healing (Kim
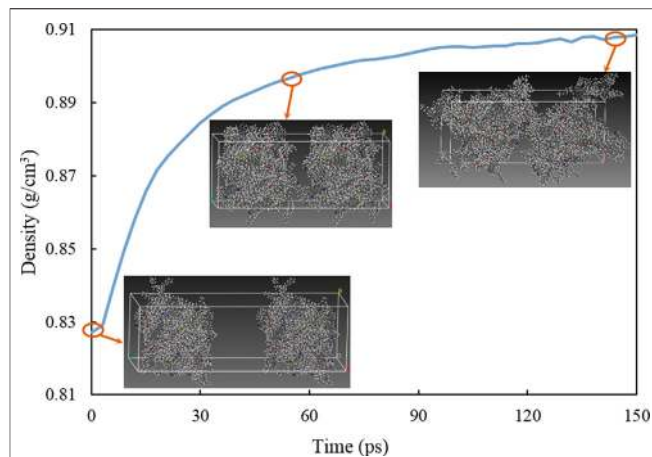
TABLE 4 | Simulated density of different asphalt binders at 25°C (Unit: g/cm^3).

Dosage (%)	CNT1	CNT2	GNF
0.5	1.014	1.015	1.011
1.0	1.016	1.018	1.012
1.5	1.011	1.020	1.004

et al., 2001a; Agzenai et al., 2015). Due to the similarity of the components, many studies on the healing phenomenon of asphalt have referred to the theories and research results in long-chain polymers, especially the asphalt self-healing processes (Ayar et al., 2015; Sun et al., 2017). At the same time, the complexities of the asphalt compositions, microstructure, and possible interactions determine the difference from long-chain polymers, which requires further research. It can be concluded from the density analysis that the diffusion process of molecules on the crack surface can be completed in a relatively short time. However, it is worth noting that the disappearance of the crack does not mean that the damage in asphalt has been repaired. The crack healing is completed in two stages: the morphological healing and the mechanical healing. Once the crack is eliminated outwardly, there are still some imperceptible voids in the crack. These voids disappear after reaching the equilibrium of molecular diffusion, thereby achieving morphological healing (Kim et al., 2001b; Qiu, 2012). In the initial stage of the asphalt molecules getting together, the entanglement of the molecules has not fully formed at the fractured interface. Therefore, a longer time is needed to the establish the molecular interaction (that is, the recovery of strength) after the morphological healing (Qiu et al., 2012).

Relative Concentration Analysis

In order to study the self-healing process of the crack in the 3D microcrack model, we mainly analyzed the relative concentration distribution along OZ direction, which was perpendicular to the
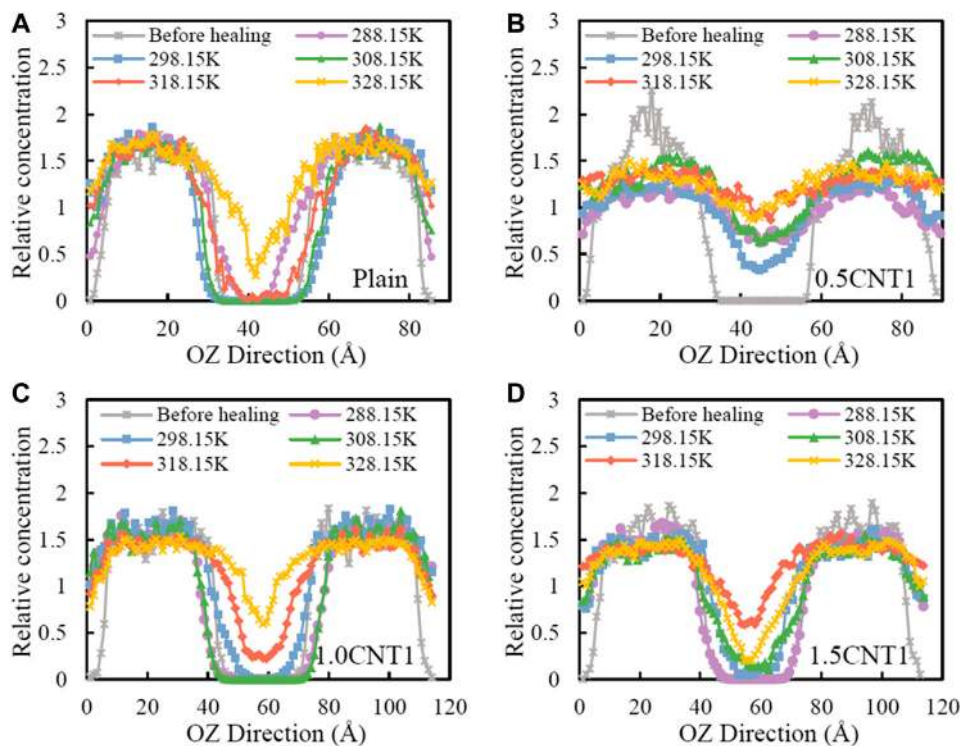
FIGURE 4 | Relative concentrations along OZ direction of the CNT1 modified PEN70 asphalt binders with different weight percentage: **(A)** plain; **(B)** 0.5% CNT1; **(C)** 1.0% CNT1; **(D)** 1.5% CNT1.

direction of the crack surface. The relative concentration distribution along OZ direction is defined as the percentage of the molecules number in the unit volume perpendicular to the direction of the crack surface. The relative concentration was obtained by calculating the density distribution of the 3D microcrack model. The relative concentration analysis simulation in Forcite module was carried out on the 3D microcrack model after the NPT ensemble simulation with 150 ps. The relative concentrations along OZ direction of the CNT1 modified PEN70 asphalt binders with different weight percentage are shown in **Figure 4**. In order to further study the effect of nanomaterials on the test results, the PEN70 asphalt binder was used as the controlled group for comparison, which was denoted as "Plain." The extremely low relative concentration in the range of about 34–54 Å (for PEN70 asphalt binder) indicated the scarce molecules in the crack area before healing. It increased particularly after healing at high temperature, meaning that the molecules got cross the crack surface and blended to each other spontaneously.

As shown in **Figure 4A**, the relative concentration values of plain PEN70 asphalt binder were near 0 in the crack area before healing. When the temperature increased, the relative concentration was gradually higher. When the temperature was 55°C, the relative concentration was less than 1.0 in the length range of 38–51 Å. In our opinion, the molecular structure was continuous without gaps when the relative concentration was

greater than 1.0, which was the average value of the relative concentrations of the CNT1 modified binder at 55°C. So, the length of the crack was reduced from 20 to 13 Å at 55°C. Generally, as the temperature decreased, the healing effect would be weakened because the molecular movement was not active according to Newton's law and the diffusion rate and range were small at low temperature. However, it was found that the concentration in the crack area at 15°C was higher than that at 25°C, which led to the higher self-healing capacity. This result was caused by the low phase transition temperature ranges of the PEN70 asphalt binder (6–18°C) (Sun et al., 2018). The asphalt suffered the phase transition process at 15°C and the molecules diffused frequently and strenuously, resulting in the self-healing of the microcracks. In the temperature range without phase transition, due to the rapid movement of molecules after absorbing heat, high temperature was the main factor that led to more effective self-healing behavior. Besides, the volume of the 3D crack model varied with the rising temperature during the NPT ensemble simulation, accompanied by the change of the length along OZ direction.

With regard to 0.5% CNT1 modified PEN70 asphalt binder, as shown in **Figure 4B**, the self-healing behavior occurred at different temperature, which was more distinct than the plain PEN70 asphalt binder. Meanwhile, the self-healing capacity varied at different temperatures and was the highest at 55°C. After adding 0.5% CNT1, the molecules could diffuse more
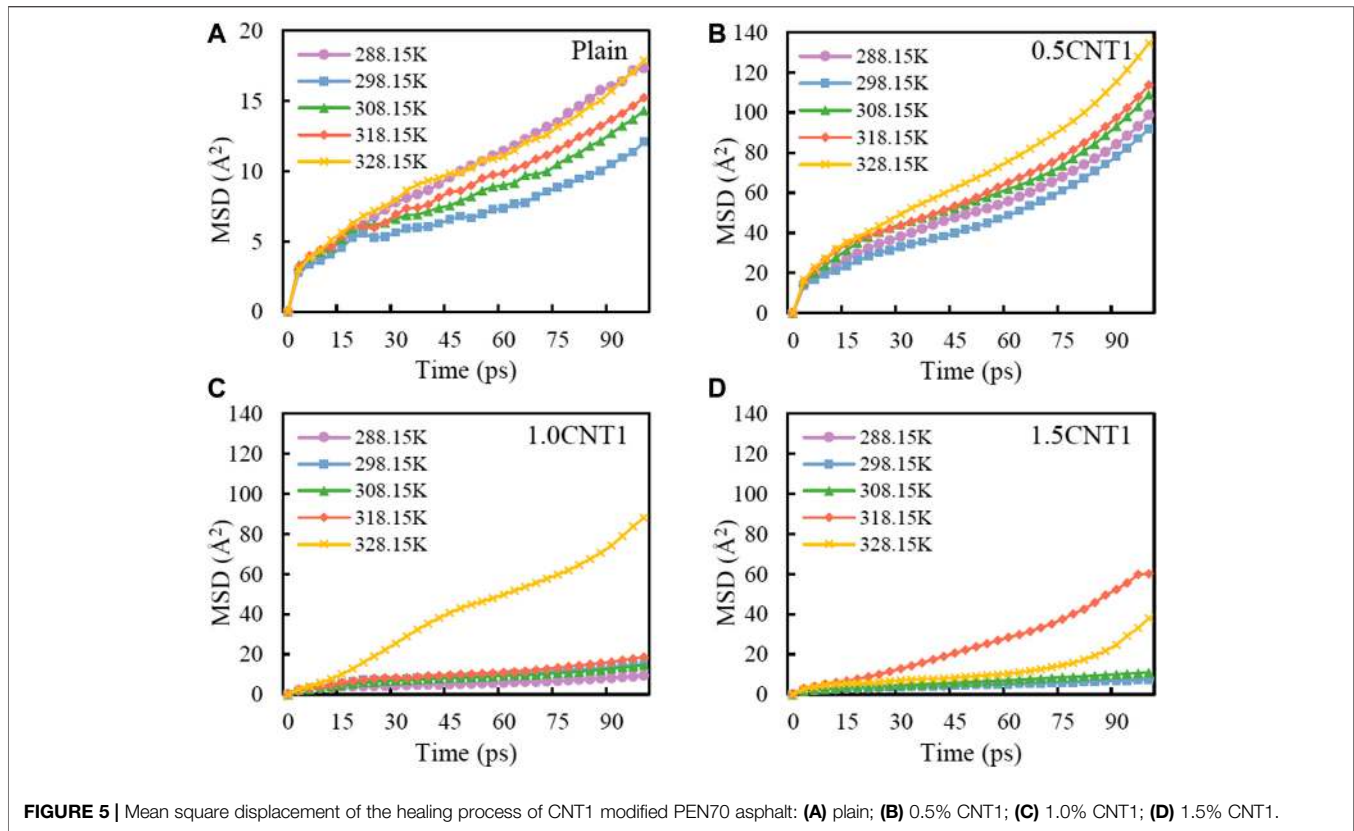
FIGURE 5 | Mean square displacement of the healing process of CNT1 modified PEN70 asphalt: **(A)** plain; **(B)** 0.5% CNT1; **(C)** 1.0% CNT1; **(D)** 1.5% CNT1.

effectively to the crack surface so that the concentration value in the crack area was close to 1.0 along the entire length at higher temperatures (above 45°C). It indicated that the microcrack was morphologically healed, while, for the 1.5% CNT1 modified PEN 70 asphalt, the most appropriate temperature for self-healing was 45°C rather than 55°C, indicating that too high temperature may be not beneficial to the healing after adding 1.5% CNT1 into the asphalt. As shown in **Figure 4D**, the length of the crack was reduced from 20 to 14 Å at 45°C, which was similar to the plain one at 55°C. Thus, it is worth noting that, when adding too much CNT1, the self-healing effect was undesirable on the contrary. In general, the self-healing of 0.5% CNT1 modified PEN 70 asphalt at different temperature was relatively obvious, and there existed an optimal weight percentage range of CNT1 for asphalt healing.

Mean Square Displacement Analysis

To study the self-healing capability of the three carbon-based nanomaterials modified PEN70 asphalt binders, the MSD analysis was conducted and the results were shown in **Figures 5–7**. In the MSD analysis, the average distances of the asphalt and nanomaterial molecules over time are measured. The value of MSD stands for the mean squared magnitude of the vector distance traveled by particle, as shown in **Eq. 1**.

$$MSD(t) = \sum_i \langle (r_i(t) - r_{i0})^2 \rangle \qquad [1]$$

where i stands for the different molecule, r_{i0} is the initial position, and $r_i(t)$ is the position vector at time t. It can be seen from **Figures 5–7** that the MSD gradually increased in the crack area at each temperature after healing and the molecules of layer-1 and layer-3 got through the vacuum layer. The self-healing of asphalt binders should be quicker when the value of MSD was larger.

CNT1 Modified PEN70 Asphalt

The MSD analysis results of the PEN70 asphalt binder are shown in **Figure 5A**. The MSD values of four binders were different at different temperatures, indicating that the healing efficiency was related to the temperature, which accorded with the practical experiment results and the analysis in *Relative Concentration Analysis*. The MSD values of the PEN70 asphalt at 15 and 55°C (near two phase transition temperatures of the PEN70 asphalt binder (Sun et al., 2018)) were stronger, while, at other temperatures, the MSD values of the PEN70 asphalt were lower. It reconfirmed that the healing ability of the asphalt was related with the phase transition temperatures. When at the temperatures range of 25–55°C, the MSD values became larger as the temperature increased. It was because the energy absorbed by the molecules was larger at the higher temperature, indicating the diffusion rate and range were high.

The CNT1 was added to the PEN70 asphalt binder at three different percentages (i.e., 0.5, 1.0, and 1.5%) of the weight of the base binder, of which the MSD analysis results are shown in **Figures 5A–D**. It showed that adding CNT1 had a noticeable increase in MSD value of modified samples especially at higher
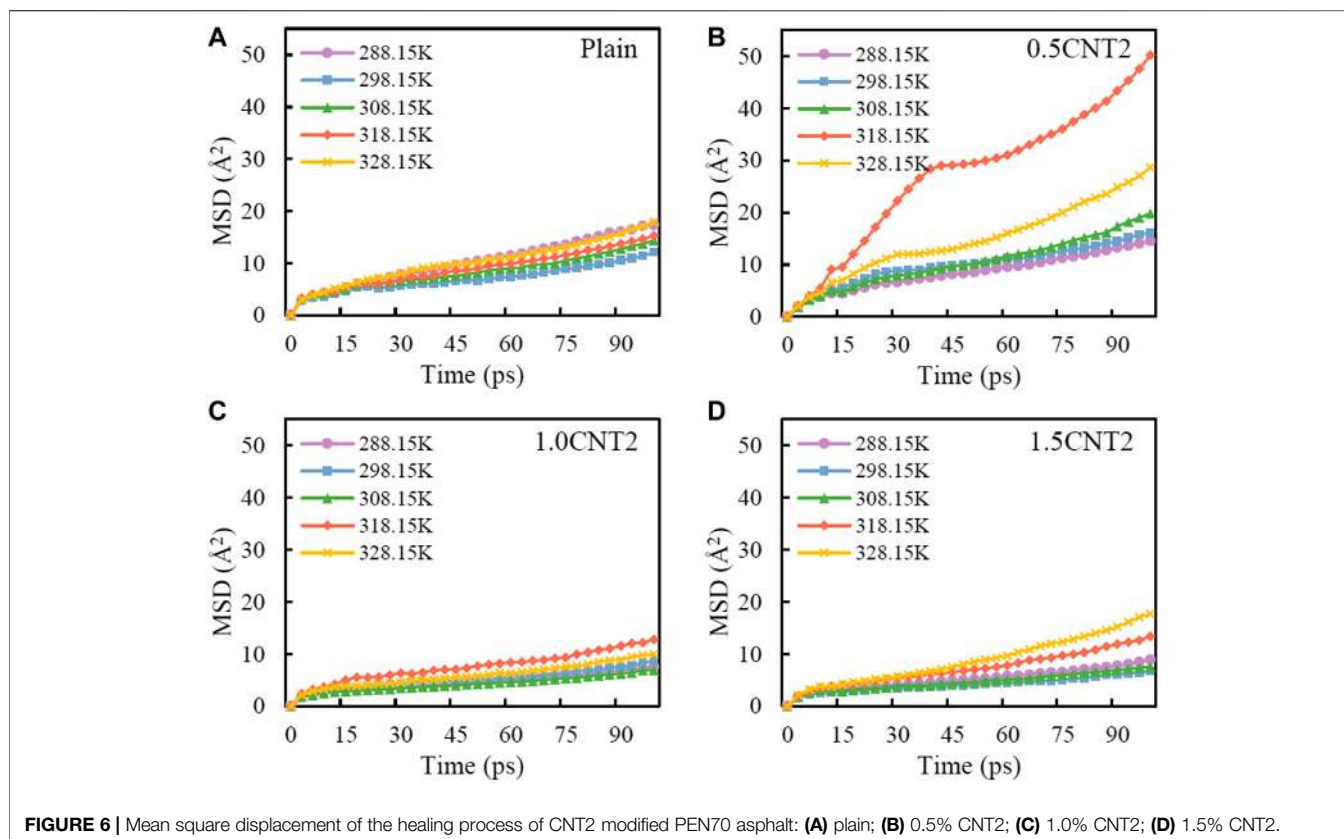
FIGURE 6 | Mean square displacement of the healing process of CNT2 modified PEN70 asphalt: **(A)** plain; **(B)** 0.5% CNT2; **(C)** 1.0% CNT2; **(D)** 1.5% CNT2.

temperatures. When the percentage of CNT1 was 0.5%, the MSD values were about five times larger than the results of the control group at the same temperatures. The above phenomena indicated that the diffusion rate and range of 0.5% CNT1 modified asphalt could be the largest, thus resulting in the best self-healing efficiency of the microcrack. It was obvious that the MSD at 45–55°C reached the larger value for the four binders; however the low phase transition temperature (15°C) was negligible when the percentage of CTN1 was more than 1.0%. It might be because the low temperature transition became unstable due to the addition of the nanomaterials. Based on this MSD analysis, considering high temperature may lead to energy dissipation and permanent deformation, the proper temperature for healing damage to asphalt binder was around 45°C and the proper dosage of CNT1 was about 0.5%, which effectively healed the cracks simultaneously.

CNT2 Modified PEN70 Asphalt

As shown in **Figure 6**, the MSD analysis of CNT2 modified PEN70 asphalt at different temperatures was conducted. Similarly, when the percentage of CNT2 was 0.5%, the MSD values were remarkable at 45°C, which meant the healing of the cracks most efficient especially around 45°C. Since the CNT1 and CNT2 had the same chemical formula but different aspect ratio, the optimal dosage for both was 0.5%, indicating that the aspect ratio has little influence on the optimal dosage of the CNT1 and CNT2. However, it was found that the more CNT2 could not

enhance the MSD value of the modified PEN70 asphalt. For instance, when at the same temperature 45°C, the MSD values of the plain group and 1.5% CNT2 modified asphalt were 17.87 and 17.66, respectively. It was deductive that adding too many CNT2 nanomaterials into the asphalt binders would result in the mixing difficulties of the composites.

GNF Modified PEN70 Asphalt

The MSD analysis results of GNF modified PEN70 asphalt at different temperature are shown in **Figure 7**. As for 0.5% GNF and 1.0% GNF modified asphalt, the difference in the MSD value was very small, and the maximum value was 18.5 and 21.6, respectively. And for 1.5% GNF modified asphalt, the distribution trend of the MSD values was basically the same at different temperatures. It can be seen that the improvement of MSD by adding GNF into the asphalt binder was limited relative to CNT. This phenomenon might be caused by the structural differentiation and the difficulties in the mixture process of the PEN70 asphalt and GNF molecules. Besides, it was reconfirmed that the phase transition at 15°C was suppressed so that the peculiar efficient diffusion and self-healing effect of the molecules disappeared.

Effect of Carbon Nanomaterials on Self-Healing Efficiency

With regard to the different dosage of nanomaterials, it was found that the CNTs modified asphalt binders respectively shown in
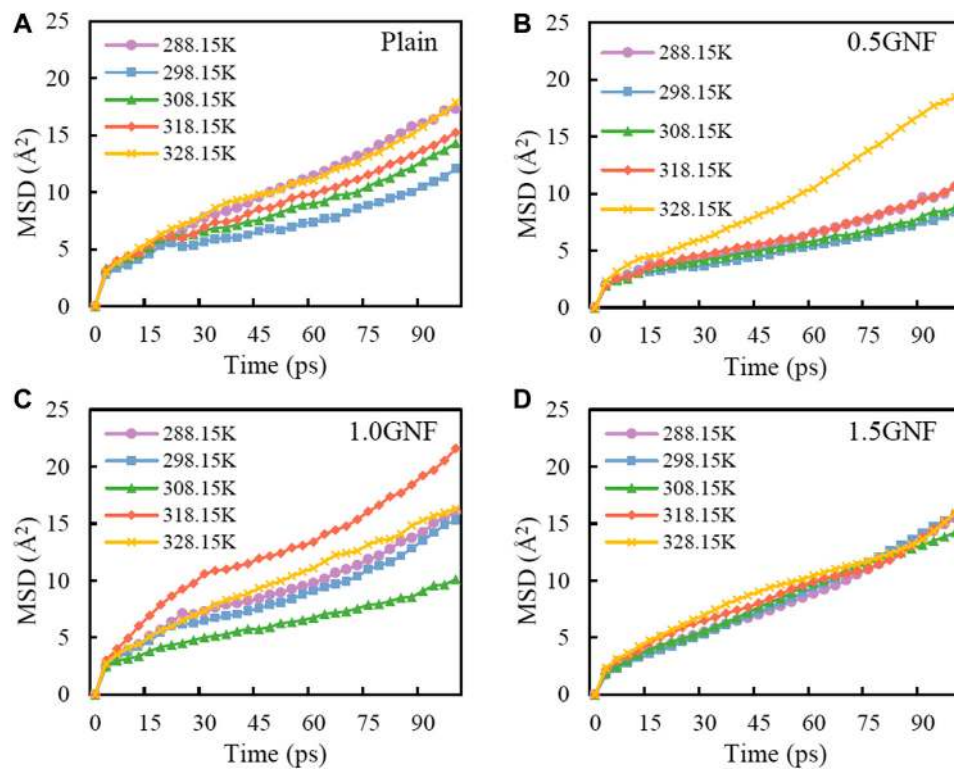
FIGURE 7 | Mean square displacement of the healing process of GNF modified PEN70 asphalt: **(A)** plain; **(B)** 0.5% GNF; **(C)** 1.0% GNF; **(D)** 1.5% GNF.
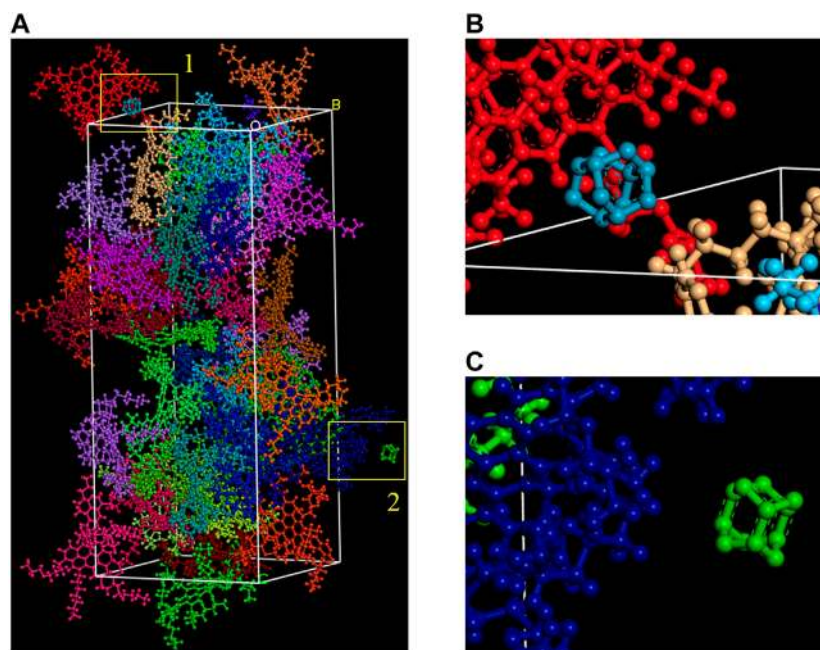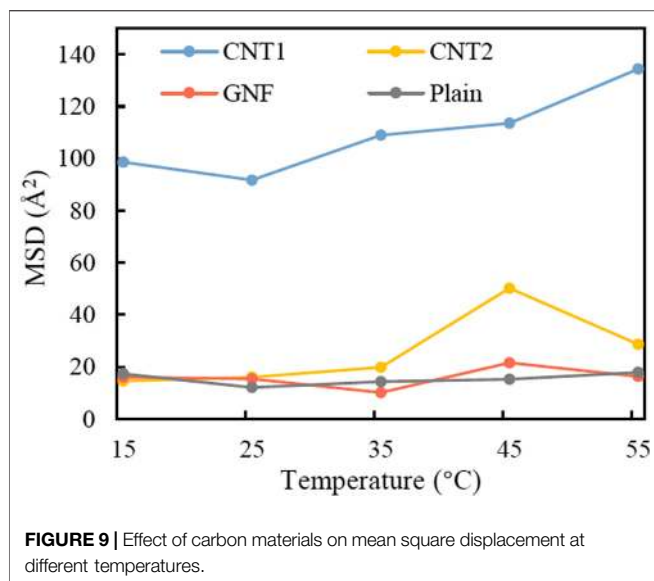

FIGURE 8 | Molecular structures of 1.0% CNT1 modified PEN70 asphalt after self-healing at 55°C: **(A)** original; **(B)** enlarged Area 1; **(C)** enlarged Area 2.

FIGURE 9 | Effect of carbon materials on mean square displacement at different temperatures.

Figures 5–7 exhibited similar healing potential tendency. When the dosage was less than 5%, the self-healing capability of all the modified asphalt binders was improved rapidly due to the addition of carbon nanomaterials. When the dosage exceeded 10%, the self-healing ability was weakened, which showed that the slope of the MSD-time curve and the final MSD value were both close to the plain group. According to the MSD simulation results, the additions of 0.5% CNT1 and CNT2 were effective in enhancing the MSD values, as well as the self-healing efficiency of plain asphalt binders. By adding 0.5% CNT1 and 0.5% CNT2, about 652% and 230% of the MSD of plain asphalt binder were enhanced at the optimal temperatures, which were 55°C and 45°C, respectively. However, the addition of GNF did not provide any noticeable changes on the MSD. In order to observe the interactions in modified asphalt binders more clearly and intuitively, the enlarged molecular structures are shown in **Figure 8**, taking 1.0% CNT1 modified PEN70 asphalt after self-healing at 55°C for example. Based on the simulation results of the MD method, the interaction strength between molecules can be judged from their distance. It can be seen from **Figure 8B** that the CNT1 molecule was very close to the long-chain branch structure of the asphalt average molecule in Area 1, indicating that strong interactions (such as entanglement) have occurred between the CNT1 and asphalt molecules. This phenomenon reproved carbon-based nanomaterials could react with the hydrophobic long-chain branches in asphalt binder and then might form more stable nanocomponents (Cheng et al., 2011; Liu et al., 2014). Moreover, the CNT1 molecule in Area 2 has been far away from the 3D molecular self-healing model, which was more frequently observed in the higher dosage of CNTs. As the dosage increased, the CNTs could not mix well with the asphalt molecules. After a period of molecular movement, the interaction between CNTs and asphalt became very weak. Thus, when too much nanomaterial was added, the effect on improving self-healing capability could be ignored. This explanation was also consistent with the simulation result that GNF and asphalt molecules were farther apart in GNF

modified asphalt binders. This was due to the inharmonious two-dimensional structure of GNF, which resulted in the difficult mixing process of asphalt binders and incorporated GNFs. Besides, the discordant GNFs might act as obstacles to reduce the diffusion of asphalt molecules at the interface, rather than promoting diffusion.

To verify the effect of carbon nanomaterials on self-healing efficiency at different temperatures, the MSD analysis of three kinds of nanomaterials at their optimal dosages are shown in **Figure 9**. For three kinds of carbon materials, the MSD reached the highest values when the temperature was in the high phase transition temperature range (45–55°C), while the low temperature transition (15°C) became negligible. It is worth noting that the phase change occurred in a temperature range, rather than a certain temperature value. So, especially with the change of adding percentage of carbon-based materials, the temperature of the maximum MSD value might change in small range. At 45–55°C, the asphalt suffered the transition from the high elastic state to the viscous flow state and released energy. Since the phase transition generated a large amount of heat, the increase of temperature was not the main factor for the improvement of self-healing efficiency in this temperature range. At this time, the molecular movement and the diffusion rate were determined by two factors in the modified asphalt system. One was the heat obtained by the molecules, and the other was the uniformity of the heat distribution. Notably, the excellent thermal conductivity of CNTs enabled the modified asphalt to rapidly reach thermal equilibrium, and all the molecules move more intensely resulting in the enhancement of the self-healing efficiency. However, the molecular diffusion rate and range did not show this especial increase at the low phase transition temperature. Meanwhile, it was also found that the self-healing capability was more obviously suppressed after adding an excessive content of nanomaterials. It is reasonable to infer that the insignificant improvement of the diffusion rate and range was due to the changes in molecular structures caused by the introduction of nanomaterials. In addition, although graphene has excellent properties, it did not significantly improve the self-healing ability of the modified asphalt binders since its molecular structure is not in harmony with the asphalt.

CONCLUSION

Aiming to evaluate the effectiveness of carbon-based nanomaterials on improving the self-healing performance of asphalt binder and to investigate the determination of the suitable type and dosage of carbon material and the selection of the optimal induction heating temperature, three different types of carbon-based nanomaterials (CNT1, CNT2 and GNF) were employed in this study. The average molecular structure models of the PEN70 asphalt binder were firstly constructed based on the measured structure parameters. Then, based mainly on MD simulations, the temperature sensitive self-healing character of damaged asphalt binders with and without carbon-based nanomaterials were quantitatively estimated under different temperature condition. Lastly, the self-healing character of asphalt binders was analyzed to determine the

suitable type and dosage of carbon material and the optimal heating temperature for self-healing.

Conclusions are listed as follows:

(1) The asphalt molecules diffused and got across the microcrack spontaneously, so that the density of the 3D cracked asphalt reached about 1.0 g/cm3 after a period of simulation time.

(2) The additions of CNTs were effective in enhancing the MSD values, as well as the self-healing efficiency of the plain asphalt binder. By adding 0.5% CNT1 and 0.5% CNT2, about 652% and 230% of the MSD of plain asphalt binder were enhanced at the optimal temperatures. Adding too much CNTs led to the undesirable self-healing effect on the contrary. However, the use of GNF as an asphalt modifier did not provide any noticeable changes on the self-healing efficiency.

(3) The self-healing capability of the asphalt was closely related to the temperature. The higher temperature resulted in the more effective self-healing. For base asphalt, the self-healing effect became especially high at the phase transition temperature range, while, for the modified asphalt, the enhancement of the self-healing capability at the low phase transition temperature (15°C) became negligible.

(4) In general, the optimal healing temperature range of the CNTs modified asphalt binders is determined as 45–55°C and the optimal dosage of the CNTs is about 0.5% over the total weight of the asphalt binder. Considering the effect of carbon-based nanomaterials on the self-healing properties, the recommended carbon-based nanomaterials modifier is CNT1 with the aspect ratio of 1.81.

DATA AVAILABILITY STATEMENT

The original contributions presented in the study are included in the article/Supplementary Material; further inquiries can be directed to the corresponding authors.

AUTHOR CONTRIBUTIONS

Conceptualization was done by YG and JX; methodology, software, formal analysis, investigation, data curation, writing, original draft preparation, review, editing, and funding acquisition were done by YG; validation was done by EY; resources were collected by EY; visualization was done by YG and JX; supervision was done by JX; project administration was done by JC; All authors have read and agreed to the published version of the manuscript.

FUNDING

ACKNOWLEDGMENTS

REFERENCES

Agzenai, Y., Pozuelo, J., Sanz, J., Perez, I., and Baselga, J. (2015). Advanced self-healing asphalt composites in the pavement performance field: mechanisms at the nano level and new repairing methodologies. *Recent Pat. Nanotechnol.* 9 (1), 43–50. doi:10.2174/1872208309666141205125017

Ayar, P., Moreno-Navarro, F., and Gámez, M. C. R. (2015). The healing capability of asphalt pavements: a state of the art review. *J. Clean. Prod.* 113, 28–40. doi:10.1016/j.jclepro.2015.12.034

Bhasin, A., Bommavaram, R., Greenfield, M. L., and Little, D. (2010). Use of molecular dynamics to investigate self-healing mechanisms in asphalt binders. *J. Mater. Civ. Eng.* 23 (4), 485–492. doi:10.1061/(ASCE)MT.1943-5533.0000200

Cheng, I. F., Xie, Y., Allen Gonzales, R., Brejna, P. R., Sundararajan, J. P., Fouetio Kengne, B. A., et al. (2011). Synthesis of graphene paper from pyrolyzed asphalt. *Carbon* 49, 2852–2861. doi:10.1016/j.carbon.2011.03.020

Du, H., and Pang, S. D. (2015a). Enhancement of barrier properties of cement mortar with graphene nanoplatelet. *Concr. Res.* 76, 10–19. doi:10.1016/j.cemconres.2015.05.007

Du, H., and Pang, S. D. (2015b). "Mechanical response and strain sensing of cement composites added with graphene nanoplatelet under tension," in *Nanotechnology in construction*. Cham, Switzerland: Springer, Cham, 377–382. doi:10.1007/978-3-319-17088-6_49

Fang, C., Yu, R., Liu, S., and Li, Y. (2013). Nanomaterials applied in asphalt modification: a review. *J. Mater. Sci. Technol.* 29, 589–594. doi:10.1016/j.jmst.2013.04.008

Faramarzi, M., Arabani, M., Haghi, A. K., and Mottaghitalab, V. (2011). "A study on the effects of CNT's on hot mix asphalt marshal-parameters," in International symposium on advances in science and technology, Iran, Bandar-Abbas, March 7–8, 2013, 1–19.

Gong, Y., Xu, J., Yan, E., Chang, R. (2020). *Intrinsic temperature and moisture sensitive adhesion characters of asphalt-aggregate interface based on molecular dynamics simulations. Constr. Build. Mater. CONBUILDMAT-D-20-03624.* (revised)

Guo, M., Liu, H., Jiao, Y., Mo, L., Tan, Y., Wang, D., et al. (2020). Effect of WMA-RAP technology on pavement performance of asphalt mixture: a state-of-the-art review. *J. Clean. Prod.* 266, 121704. doi:10.1016/j.jclepro.2020.121704

Katayama, Y., Hosoi, T., and Takeya, G. (1975). Structural analysis of coal tar pitches and petroleum heavy oil distillation residues using a computer. *Nippon Kagaku Kaishi* 1, 127–134. doi:10.1246/nikkashi.1975.127

Kim, Y. R., Lee, H., and Little, D. N. (2001a). "Microdamage healing in asphalt and asphalt concrete," in *Volume IV: A viscoelastic continuum damage fatigue model of asphalt concrete with microdamage healing.* College Station, TX: Texas Transportation Institute.

Kim, Y. R., Little, D. N., and Lytton, R. L. (2001b). Evaluation of microdamage, healing, and heat dissipation of asphalt mixtures, using a dynamic mechanical analyzer. *J. Trans. Res. Rec.* 1767 (1), 60–66. doi:10.3141/1767-08

Latifi, H., and Hayati, P. (2018). Evaluating the effects of the wet and simple processes for including carbon nanotube modifier in hot mix asphalt. *Constr. Build. Mater.* 164, 326–336. doi:10.1016/j.conbuildmat.2017.12.237

Lee, S.-J., You, I., Zi, G., and Yoo, D.-Y. (2017). Experimental investigation of the piezoresistive properties of cement composites with hybrid carbon fibers and nanotubes. *Sensors* 17 (11), 2516–2531. doi:10.3390/s17112516

Liu, Q., Schlangen, E., van de Ven, M., van Bochove, G., and van Montfort, J. (2012). Evaluation of the induction healing effect of porous asphalt concrete through four point bending fatigue test. *Constr. Build. Mater.* 29: 403–409. doi:10.1016/j.conbuildmat.2011.10.058

Liu, Z., Tu, Z., Li, Y., Yang, F., Han, S., Yang, W., et al. (2014). Synthesis of three-dimensional graphene from petroleum asphalt by chemical vapor deposition. *Mater. Lett.* 122, 285–288. doi:10.1016/j.matlet.2014.02.077

Maginn, E. J., and Elliott, J. R. (2010). Historical perspective and current outlook for molecular dynamics as a chemical engineering tool. *Ind. Eng. Chem. Res.* 49 (7), 3059–3078. doi:10.1021/ie901898k

Novoselov, K. S., Geim, A. K., Morozov, S. V., Jiang, D., Zhang, Y., Dubonos, S. V., et al. (2004). Electric field effect in atomically thin carbon films. *Science* 306, 666–669. doi:10.1126/science.1102896

Qiu, J. (2012). *Self healing of asphalt mixtures: towards a better understanding of the mechanism.* Delft, Netherlands: TU Delft, Delft University of Technology.

Qiu, J., Van de Ven, M., Wu, S., Yu, J., and Molenaar, A. (2012). Evaluating self healing capability of bituminous mastics. *Exper. Mech.* 52 (8), 1163–1171. doi:10.1007/s11340-011-9573-1

Shen, J. A. (2011). *Pavement performance of asphalt and asphalt concrete.* Beijing, China: China Communication Press. [in Chinese, with English summary].

Steyn, W. J. (2009). Potential applications of nanotechnology in pavement engineering. *J. Transp. Eng.* 135, 764–772. doi:10.1061/(asce)0733-947x(2009)135:10(764)

Su, J.-F., Guo, Y.-D., Xie, X.-M., Zhang, X.-L., Mu, R., Wang, Y.-Y., et al. (2019). Smart bituminous material combining anti-icing and self-healing functions using electrothermal graphene microcapsules containing oily rejuvenator. *Constr. Build. Mater.* 224, 671–681. doi:10.1016/j.conbuildmat.2019.07.098

Sun, D., Sun, G., Zhu, X., Pang, Q., Yu, F., and Lin, T. (2017). Identification of wetting and molecular diffusion stages during self-healing process of asphalt binder via fluorescence microscope. *Constr. Build. Mater.* 132, 230–239. doi:10.1016/j.conbuildmat.2016.11.137

Sun, D., Sun, G., Zhu, X., Ye, F., and Xu, J. (2018). Intrinsic temperature sensitive self-healing character of asphalt binders based on molecular dynamics simulations. *Fuel* 211, 609–620. doi:10.1016/j.fuel.2017.09.089

Wang, H., Lin, E., and Xu, G. (2017). Molecular dynamics simulation of asphalt-aggregate interface adhesion strength with moisture effect. *Inter. J. Pav. Eng.* 18 (5), 414–423. doi:10.1080/10298436.2015.1095297

Wang, Z., Dai, Q., Porter, D., and You, Z. (2016). Investigation of microwave healing performance of electrically conductive carbon fiber modified asphalt mixture beams. *Constr. Build. Mater.* 126, 1012–1019. doi:10.1016/j.conbuildmat.2016.09.039

Xu, G., and Wang, H. (2017). Molecular dynamics study of oxidative aging effect on asphalt binder properties. *Fuel* 188, 1–10. doi:10.1016/j.fuel.2016.10.021

Yao, H., Dai, Q., and You, Z. (2016). Molecular dynamics simulation of physicochemical properties of the asphalt model. *Fuel* 164, 83–93. doi:10.1016/j.fuel.2015.09.045

Yao, H., You, Z., Li, L., Lee, C. H., Wingard, D., Yap, Y. K., et al. (2013). Rheological properties and chemical bonding of asphalt modified with nanosilica. *J. Mater. Civil Eng.* 25 (11), 1619–1630. doi:10.1061/(asce)mt.1943-5533.0000690

Yildirim, Y. (2007). Polymer modified asphalt binders. *Construct. Build. Mater.* 21, 66–72. doi:10.1016/j.conbuildmat.2005.07.007

Yoo, D. Y., Kim, S., Kim, M.-J., Kim, D., and Shin, H.-O. (2019). Self-healing capability of asphalt concrete with carbon-based materials. *J. Mater. Res. Technol.* 8 (1), 827–839. doi:10.1016/j.jmrt.2018.07.001

Yoo, D. Y., You, I., and Lee, S.-J. (2018). Electrical and piezoresistive sensing capacities of cement paste with multi-walled carbon nanotubes. *Arch. Civil Mech. Eng.* 18 (2), 371–384. doi:10.1016/j.acme.2017.09.007

Young, R. J., Kinloch, I. A., Gong, L., and Novoselov, K. S. (2012). The mechanics of graphene nanocomposites: a review. *Compos. Sci. Technol.* 72, 1459–1476. doi:10.1016/j.compscitech.2012.05.005

Zare-Shahabadi, A., Shokuhfar, A., and Ebrahimi-Nejad, S. (2010). Preparation and rheological characterization of asphalt binders reinforced with layered silicate nanoparticles. *Constr. Build. Mater.* 24 (7), 1239–1244. doi:10.1016/j.conbuildmat.2009.12.013